Analysis of material dependency in an elastic - plastic contact models using contact mechanics approach

V.C. Sathish Gandhi[*1], R. Kumaravelan[2a], S. Ramesh[3b] and K. Sriram[4c]

[1]*Department of Mechanical Engineering, University College of Engineering Ariyalur (A constituent College of Anna University, Chennai), Ariyalur - 621 704, Tamilnadu, India*
[2]*Department of Mechanical Engineering, Velalar College of Engineering and Technology, Erode - 638 012, Tamilnadu, India*
[3]*Department of Mechanical Engineering,Vel Tech High Tech Dr.Rangarajan Dr.Sakunthala Engineering College, Chennai - 600 062, Tamilnadu, India*
[4]*Department of Mechanical Engineering, Amrita School of Engineering, Coimbatore - 641 112, Tamilnadu, India*

Abstract. The study aims on the effect of material dependency in elastic- plastic contact models by contact analysis of sphere and flat contact model and wheel rail contact model by considering the material properties without friction. The various materials are selected for the analysis based on Young's modulus and yield strength ratio (*E/Y*). The simulation software 'ANSYS' is employed for this study. The sphere and flat contact model is considered as a flattening model, the stress and strain for different materials are estimated. The simulation of wheel-rail contact model is also performed and the results are compared with the flattening model. The comparative study has also been extended for finding out the mean contact pressure for different materials the *E/Y* values between 150 and 660. The results show that the elastic-plastic contact analysis for materials up to *E/Y*=296.6 is depend on the nature of material properties and also for this material the mean contact pressure to yield strength reaches 2.65.

Keywords: contact analysis; *E/Y* ratio; stress; strain; mean contact pressure; yield strength

1. Introduction

Contact mechanics is the study of the deformation of solids that touch each other at one or more points. The theory developed by Hertz (1881) remains the foundation for most contact problems encountered in engineering. It applies to normal contact between two elastic solids that are smooth and can be described locally with orthogonal radii of curvature such as a toroid. Further, the size of the actual contact area must be small compared to the dimensions of each body and to the radii of curvature. Hertz made the assumption based on the observations that the contact

---

∗Corresponding author, Assistant Professor, E-mail: vcsgandhi@gmail.com
[a]Professor, E-mail: rkumaravelan@gmail.com
[b]Professor, E-mail: ramesh_1968in@yahoo.com
[c]Assistant Professor, E-mail: srk.sriramk@gmail.com

area is elliptical in shape for such three-dimensional bodies.

2. Theoretical background

In a sphere and flat contact model, sphere is to be considered as a deformable body and flat as a rigid member. This type model is available in the roller guide ways, roller bearings, wheel and rail contact and cam mechanism. In this type of models the sphere is pressed against a rigid flat when load is applied on the top surface of the sphere. When the load is applied initially a point contact is obtained then slowly it is changed as a circular surface contact. The deformed material is mount up in the sphere only. When the deformation is more, the material tends to fail. The contact condition between the wheel and rail contact, the contact zone surfaces and bulk material must be strong to resist the heavy loads and dynamic response. The contact zone must be small compared with the overall dimensions and its shape of the wheel and rail.

3. Literature review

Contact analysis can be traced back to 1882, in which Hertz studied the elastic contact between two glass lenses. The Hertz theory is restricted to the normal frictionless contact between an elastic half-space with small deformation. CEB model (Chang *et al*. 1987) has been developed on volume conservation of the plastically deformed asperities for an elastic-plastic contact model. Kogut and Etison (2002) (KE model) used the constitutive laws appropriate to any mode of deformation, be it elastic or plastic using Finite element method solution for the elastic-plastic contact of a deformable sphere and a rigid flat without considered the material properties. Jackson and Green (2005) (JG model) presented some empirical relations of contact area and contact load with considered the material properties and the geometry of contacting body. Polin and Lin (2006) developed a new method to determine the elasto-plastic regime of a spherical asperity in terms of the interference of two contact surfaces. Monfared (2012) presented the contact stress analysis in rolling bodies by finite element method to analyse the pressure of collection of the wheel and rail, elliptical, rectangular and circular contact surfaces are assumed for this study using classical mechanics approach. Zakeri *et al*. (2011) studied the effect of geometrical parameters on the behaviour of dynamic interaction of wheel-rail is being investigated through a parametric study. Zong *et al*. (2012) analyzed a three-dimensional wheel – rail contact model in the finite element framework is used for the analysis of the rail ends under wheel contact loading. Zhu *et al*. (2007) studied an adaptive wheel-rail contact model with radial spring is developed for prediction of wheel-rail normal contact force. Arslan and Kayabasi (2012) has presented the fundamental way of handling Rail-Wheel contact problems from the FEA standpoint, and highlighted the required steps for more realistic 3D solutions to these types of problems. Mohan (2012) has studied the applications of railway wheel viz., the behaviour of wheel subjected to thermal and structural loading and the combined loading. He pointed out that an excessive braking of wheel leads to thermal overloading which results in fatigue, crack propagation leading to fracture and wear. Santamaria *et al*. (2009) presented a wear index prediction for wheel-rail contact model of multiple contact patches for the two contact point situation using three-dimensional analysis of surfaces including the influence of the angle of attack. In these cases the front wheel set's angle of attack tends to adopt high values that have a considerable effect on the localisation of contact patches,

increasing creep and wear indices. Braghin *et al.* (2006) proposed a mathematical model to predict a railway wheel profile evaluation due to wear. Donzella and Petrogalli (2010) proposed a failure assessment diagram for the evaluation of the safe working area of components subjected to rolling contact loading. The rolling contact fatigue limitation in terms of non-propagation condition of inherent defects. Static fracture and ratchetting limitations are also added to the diagram. Sathish Gandhi *et al.* (2012) presented the effect of tangent modulus in a contact parameters of a spherical ball contact with a flat plate. The different materials are considered for the study between *E/Y*=500 and 1750. Monfared (2011) has proposed a new formulation of contact stress for two rolling bodies is presented, and its results are close to the hertz stress formulation. The analysis of stress, fracture, prediction of fracture and path of crack motion in rail and wheel are studied statically. Yaylac and Birinci (2013) studied the contact problem of two elastic layers with elastic constant and different height are considered for analysis. Monfared and Khalili (2011) presented the mechanical behaviour of the one Lead-Zirconate-Titanate by its atomic number and its certain mechanical behaviour is simulated by the mathematical modeling and ABAQUS software for smart materials, as well as prediction of mechanical behaviours. Kumaravelan *et al.* (2013) has discussed the design and contact analysis of leaf spring for two different cases such as single cantilever solid triangle beam and 3-beams of rectangular cross section for different materials.The detail reviewed shows that the material dependency of elastic-plastic of sphere and flat model is not discussed and the wheel- rail contact analysis pointed out the wear calculation, failure analysis ect. The material dependency analysis are not pointed out in the literature review.

4. Materials and methods

A Finite Element model of a sphere and flat contact model has been developed in ANASYS 10. As to improve an efficiency of analysis the 2D axis symmetric model is created. The Fig. 1 shows the model of sphere and flat.

The present two-dimensional analysis aims to study the contact stress and strain for different *E/Y* values of material, under the loading condition of the sphere and flat contact model. Table 1 shows the materials used for the applications of contact problems for different yield strength. Take $E=2.15\times10^5$ N/mm^2.

Fig. 2 shows basic model in which sphere is modeled using one quarter of circle of radius 50.02mm and the rigid flat is represented as a straight line. A two dimensional, 8-node,
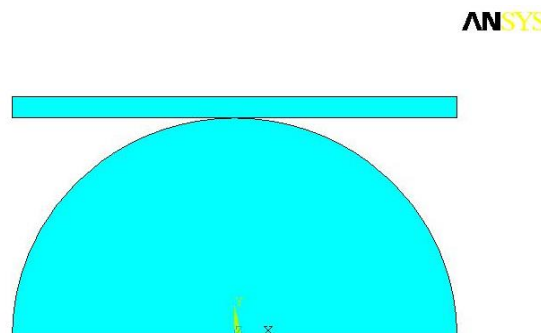
ANSYS

Fig. 1 Sphere and flat model

Table 1 Material properties

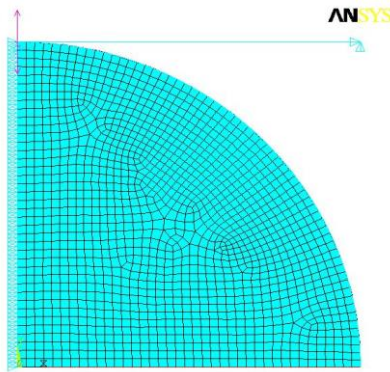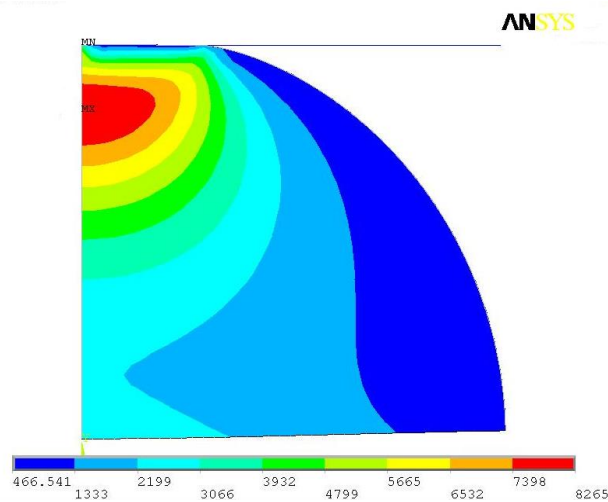| S. No.	Y N/mm^2	E/Y
1	1433.33	150
2	724.88	296.6
3	591.31	363.6
4	457.45	470
5	398.15	540
6	325.76	660

Fig. 2 Sphere and flat model (Boundary conditions)

Fig. 3 Plot for stress distribution (E/Y=150)

quadrilateral, and axis symmetric solid PLANE82 element is used for modeling. Higher order surface-surface contact element is used to create the contact between the sphere and flat plate. TARGET 169 and CONTA 172 are employed in this modeling. The flat is rigid body so that all degrees of freedom are arrested and the radial movement of the sphere is also restricted to move in this direction. The sphere has allow to move in the vertical direction only and the load is applied in the bottom of hemisphere.
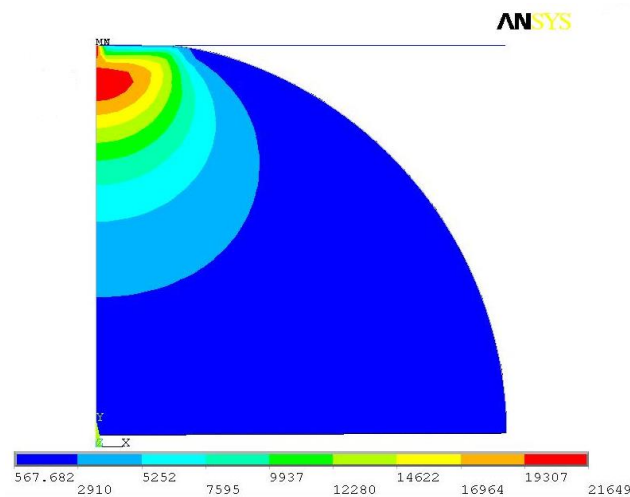
Fig. 4 Plot for stress distribution (*E/Y*=660)
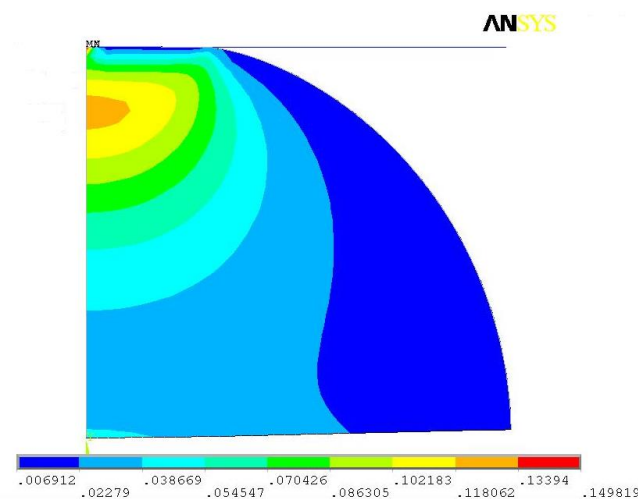
Fig. 5 Plot for strain distribution (*E/Y*=150)

4.1 Analysis of stress distribution for different materials

The finite element simulation has been performed for different *E/Y* values of material such as 150, 296.6, 363.6, 470, 540, 660. The analysis has been carried out for these materials based on contact stress. The stress distribution are plotted for a load (Pressure) of 780 N/mm^2. The plots are given for the minimum and maximum value of *E/Y*.

Fig. 3 shows the stress distribution of material (*E/Y*=150) in which the maximum and minimum stress value are 8265 N/mm^2 and 466.541 N/mm^2 respectively. It is observed that the maximum stress is developed in the underneath of the contact region.

Fig. 4 shows the stress distribution of material (*E/Y*=660) in which the maximum and minimum stress values are 21649 N/mm^2 and 567.682 N/mm^2 respectively. It is observed that the stress distribution is move towards the contact region if the *E/Y* value of the material increases.
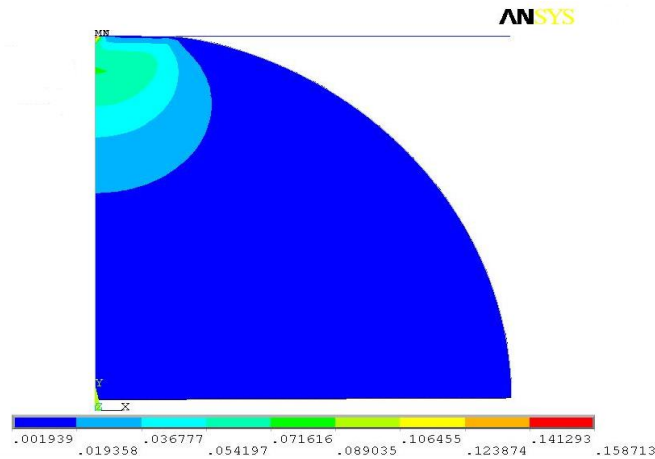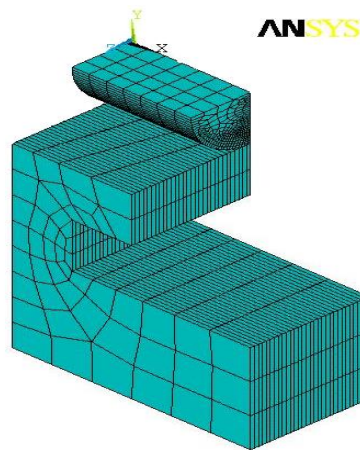
Fig. 6 Plot for strain distribution (*E/Y*=660)

Fig. 7 Finite element contact model of a wheel and rail (3D)

4.2 Analysis of strain distribution for different materials

The finite element simulation has been performed for different *E/Y* values of material such as 150, 296.6, 363.6, 470, 540, 660. The analysis has been carried out for these materials based on strain developed in the model. The strain distribution are plotted for a load (Pressure) of 780 N/mm^2. The plots are given for the minimum and maximum value of *E/Y*.

Fig. 5 shows the strain distribution of material (*E/Y*=150) in which the maximum and minimum strain values are 0.149819 and 0.006912 respectively. Fig. 6 shows the strain distribution of material (*E/Y*=660) in which the maximum and minimum strain values are 0.158713 and 0.001939 respectively.

4.3 Analysis of a wheel-rail contact

The finite element analysis software 'ANSYS' has been used to carry out this analysis, in an

axisymmetric condition. Hence, a quarter wheel (cylinder) is considered for the analysis. The 3D finite element contact model of a wheel and rail is shown in Fig. 7.

For this contact model the contact pair is created and confirmed between the wheel and rail as shown in Fig. 7. The dimensions of the model are as follows: diameter of the wheel is 10 mm and wheel thickness is 20 mm. Rail dimensions are: base width is 40 mm; head width is 20 mm; head thickness is 5 mm; and rail height is 20 mm; length of the rail is 20 mm.

For this investigation both wheel and rail are discretized by eight-noded brick 185 element. The upper surface of rail is selected as target surface (target 169) and curved surface of wheel is selected as contact surface (conta 172). The nodes lying on the axis of the wheel and rail are restricted to move in the radial direction. Also the nodes in the bottom of the rail are fixed in all the directions. The average wheel size used for this analysis is 5 mm radius. The material properties are selected based on the Young's modulus to yield strength ratio (1999). The load is applied as a constant pressure of 0.5 MPa on the top surface of the wheel. The different Young's modulus to yield strength ratio is considered for analysis between 100 and 700. The *E/Y* ratio is considered for this analysis is less than 1000 for high yield strength of the material. The finite element simulation has been performed for different *E/Y* values of material such as 150, 296.6, 363.6, 470, 540, 660. The performance study has been carried out for these materials based on contact stress and strain.

4.3.1 Analysis of stress distribution (Wheel-rail model)

The analysis is performed for different materials having *E/Y* value between 100 and 700. The load is applied in the top surface of the wheel in terms of constant pressure of 0.5 MPa. Initially the contact is of a point contact, then it is a line contact after load is applied. The distribution of stress has been estimated between the wheel and rail. The stress distribution plots are given for the minimum and maximum values of *E/Y* ratios.

Fig. 8 shows the stress distribution for the material (*E/Y*=150) for wheel and rail contact model. The Maximum stress of 3448 N/mm² is developed at the edge of the contact area for this material. It is observed that for low *E/Y* value of material the maximum stress is developed at the edge of the contact.
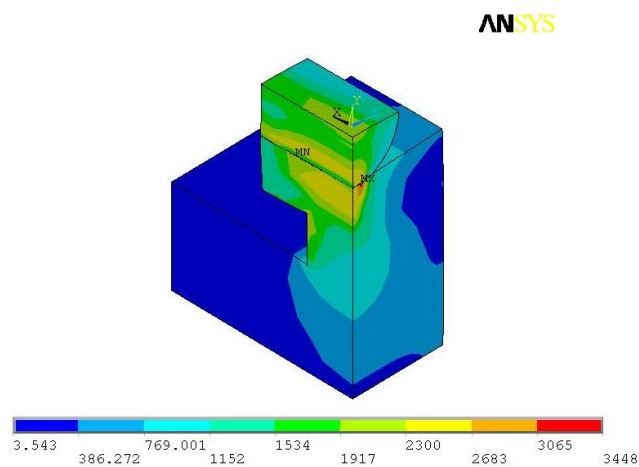

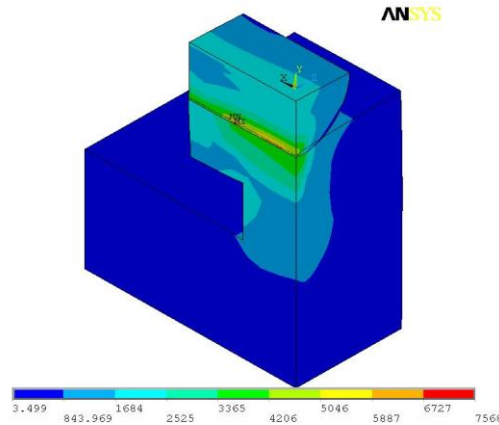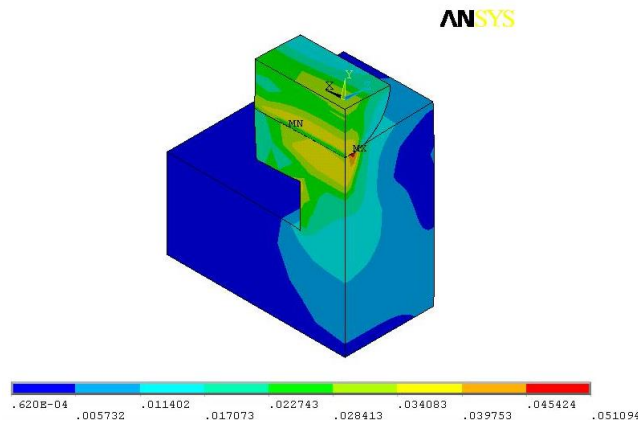Fig. 8 Plot for strain distribution for the material *E/Y*=150

Fig. 9 Plot for strain distribution for the material *E/Y*=660

Fig. 10 Plot for strain distribution for the material *E/Y*=150

Fig. 9 shows the stress distribution for the material (*E/Y*=660) for wheel and rail contact model. The Maximum stress of 7568 N/mm^2 is developed at the center of the line of contact for this material. It is observed that for high *E/Y* value of material the maximum stress is developed at the center of the line of contact.

4.3.2 Analysis of strain distribution (Wheel - rail model)

The strain analysis has been carried out for the wheel and rail contact model for different materials. The strain distribution plots are given for the minimum and maximum values of *E/Y* ratios.

Fig. 10 shows the strain distribution for the material (*E/Y*=150) for wheel and rail contact model. The Maximum strain of 0.051094 is developed at the edge of the contact for this material.

Fig. 11 shows the strain distribution for the material (*E/Y*=660) for wheel and rail contact model. The Maximum strain of 0.025897 is developed at the center of line of contact for this material. It is observed that for the low *E/Y* of material the maximum strain is developed at the edge of the contact and for high *E/Y* value of material the maximum strain is migrated into the center of the line of contact between the wheel and rail.
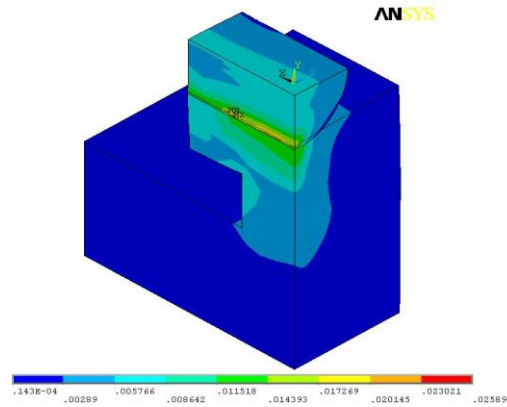
Fig. 11 Plot for strain distribution for the material *E/Y*=660

5. Studies of various flattening approach contact models

The comparison has been made for various flattening approach contact model such as Chang - Etsion - Bogy (CEB model), Kogut - Etison (KE model), Jackson and Green (JG model) and Li Polin and Jen Fin Lin (LJ model). The main objective of this study is to find out the material distinguishing of elastic-plastic model in the contact analysis based on the mean contact pressure.

5.1 CEB-Model

CEB model developed an elastic-plastic contact model based on volume conservation of the plastically deformed asperities. From the work of Tabor (1951) it can be shown that initial yield occurs in this model when mean contact pressure, P_m=0.6H where H is the hardness of the softer material. For a more generated representation, the maximum contact pressure of the inception of plastic deformation to the hardness by

$$P_m = kH \tag{1}$$

5.2 KE-Model

Finite element method solution for the elastic-plastic contact of a deformable sphere and a rigid flat by using constitutive laws appropriate to any mode of deformation, be it elastic or plastic. It also offers a general dimensionless solution not restricted to a specific material or geometry. In this method, the plastic region evolution inside the sphere, if increasing interference value upto110. i.e., $\dfrac{\omega}{\omega_c}=110$. The plastic region is completely surrounded by a elastic material, at interference value up to 6. i.e., $\dfrac{\omega}{\omega_c}=6$.

The empirical expressions obtained from the curve fitting for the mean contact pressure in the above three stages.

Table 2 Stress and strain distribution - Fattening model (FE - analysis)

S. No	E/Y value	Stress (N/mm^2)	Strain (N/mm^2)
1	150	8265	0.149819
2	296.6	10985	0.178477
3	363.6	9161	0.164535
4	470	11377	0.160279
5	540	12280	0.169979
6	660	21649	0.158713

$$\frac{p}{Y} = 1.19 \left(\frac{\omega}{\omega_c} \right)^{0.289} \quad \text{for} \quad 1 \le \omega/\omega_c \le 6 \tag{2}$$

$$\frac{p}{Y} = 1.61 \left(\frac{\omega}{\omega_c} \right)^{0.117} \quad \text{for} \quad 6 \le \omega/\omega_c \le 110 \tag{3}$$

5.3 JG-Model

JG-model used the finite element method to model the case of an elastic-perfectly plastic sphere in frictionless contact with a rigid flat. The JG- model considered only three different *E/Y* values like 250, 166.67 and 125 which elastic-plastic transition starts based on the evolution of elastic core. The average pressure to yield strength ratio, *P/AY* can now be formulated as

$$P/AY = \frac{2}{3} C \frac{P^*}{A^*} \tag{4}$$

5.4 LJ-Model

This model is developed to determine the elasto-plastic regime of a spherical asperity in terms of the interference of two contact surfaces. This method provides an efficient way to solve the problem of discontinuities often present in the reported solutions for the contact load and area or the gradients of these parameters obtained at either the inception or the end of the elasto-plastic regime. The dimensionless average contact pressure (P_{ave}/Y) of an asperity for the Rigid Flat (RF) case is calculated by this method. After adjustments in RF cases, the average contact pressure is expressed as

$$P_{ave}\Big/ Y = 1.08 \exp\left[0.559 \ln\left(\omega/\omega_{ec}\right) - 0.1232 \left(\ln\left(\omega/\omega_{ec}\right)\right)^2 + 0.0095 \left(\ln\left(\omega/\omega_{ec}\right)\right)^3 \right] \tag{5}$$
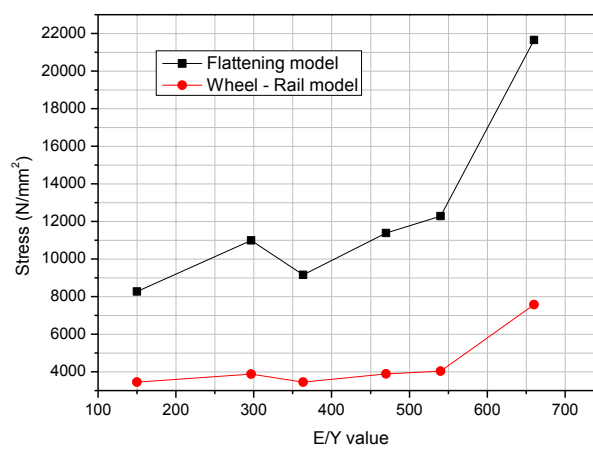
$$\text{at} \quad 1 \le \delta/\delta_{ec} \le 80$$

6. Result and discussion

The flattening model and wheel - rail model contact simulation has been performed for

Table 3 Stress and strain distribution - wheel rail model (FE - analysis)

S. No	*E/Y* value	Stress (N/mm^2)	Strain
1	150	3448	0.051094
2	296.6	3880	0.05698
3	363.6	3722	0.041733
4	470	3886	0.03528
5	540	4033	0.034863
6	660	7568	0.025897

Fig. 12 *E/Y* value Vs Stress distribution
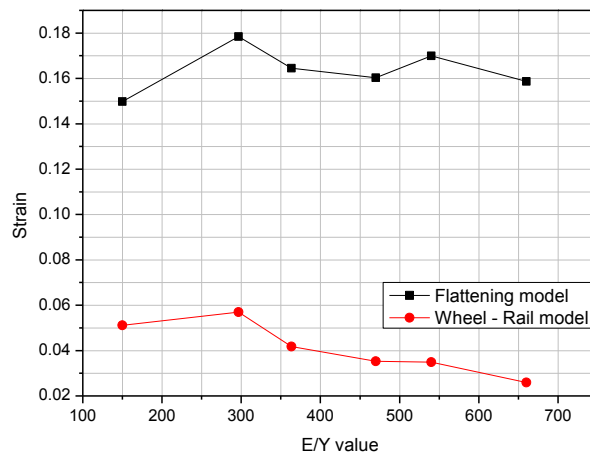
Fig. 13 *E/Y* value Vs Stress distribution

different materials using the analysis software 'ANSYS'. The results were obtained from the simulations and analytical study are discussed as follows:

The stress and strain distribution in flattening model has been performed for different *E/Y* values. Table 2 shows the stress distribution values for different *E/Y* values of materials.

Table 2 shows that if the *E/Y* value increases the stress and strain increases and further increase in *E/Y* value stress and strain decreases again increases for further increase in *E/Y* value.

The stress and strain distribution in wheel-rail model has been performed for different *E/Y* values. Table 3 shows the stress distribution values for different *E/Y* values of materials.

Table 2 shows that if the *E/Y* value increases the stress and strain increases and further increase in *E/Y* value stress and strain decreases again increases for further increase in *E/Y* value.

Fig. 12 shows the relation between *E/Y* value of material and stress distribution in the flattening and wheel-rail models. It is observed that upto *E/Y*=296.6 the stress distribution is increased after that it is decreased, similarly the stress increases with the *E/Y* value of material increases.

Fig. 13 shows the relation between *E/Y* value of material and strain distribution in the flattening and wheel-rail models. It is observed that upto *E/Y*=296.6 the strain distribution is increased and then decreased similarly it increases if the *E/Y* value of material increases.

6.1 Comparison of CEB, KE and LJ Models

The mean contact pressure is expressed as a function of dimensionless interference ratio (ω/ω_c) and *E/Y* ratio. An analytical work was carried out for the p/Y value. From the CEB-model the mean contact pressure to yield strength value is calculated. CEB model assumes abrupt transition from elastic deformation to fully plastic flow of asperity. In this model the upper limit of contact pressure is hardness coefficient (*K*). The mean contact pressure (p_m) to yield strength ratio (*p/Y*) in CEB model is equal to KH where H is the hardness of the soft material is equal to 2.8Y

$$p_m = KH$$

$$= (0.454 + 0.41\nu)\,2.8Y$$

$$\frac{p_m}{Y} = 1.64$$

From the KE-model in Eq. (2) the values of mean contact pressure to yield strength ratio are also calculated and shown in the Table 4 upto an interference value of inception of fully plastic regime; ω/ω_c=80. In the KE-model, the p/Y value is independent of material properties. From the LJ-model in rigid flat case in Eq. (5) the values of mean contact pressure to yield strength ratio are

Table 4 Dimensionless interference and p/Y ratio (KE and LJ - models)

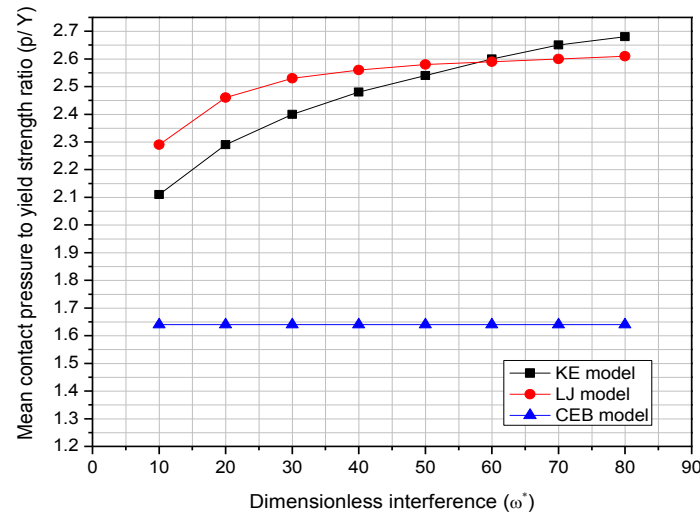| S. No.	$\omega^* = \dfrac{\omega}{\omega_c}$	P/Y	
		KE - model	LJ - model
1	10	2.11	2.29
2	20	2.29	2.46
3	30	2.40	2.53
4	40	2.48	2.56
5	50	2.54	2.58
6	60	2.60	2.59
7	70	2.65	2.60
8	80	2.68	2.61

Fig. 14 Mean contact Pressure to Yield strength ratio Vs Dimensionless interference

Table 5 Dimensionless interference and p/Y ratio of different materials

S. No.	Dimensionless interference $\omega^* = \dfrac{\omega}{\omega_c}$	Mean contact pressure to Yield strength ratio, p/Y					
		E/Y					
		150	296.6	363.6	470	540	660
1	10	2.17	2.18	2.19	2.18	2.144	2.23
2	20	2.39	2.42	2.44	2.44	2.408	2.498
3	30	2.48	2.54	2.57	2.57	2.53	2.63
4	40	2.52	2.61	2.64	2.67	2.61	2.707
5	50	2.53	2.63	2.69	2.7	2.66	2.756
6	60	2.53	2.64	2.71	2.73	2.7	2.79
7	70	2.53	2.65	2.72	2.76	2.731	2.81
8	80	2.52	2.65	2.73	2.77	2.74	2.831

calculated and shown in the Table 3 upto an interference value of inception of fully plastic regime; ω/ω_c=80.

From Table 4 it can be seen that, the p/Y ratio of KE-model reaches up to 2.68 at the inception of fully plastic regime without considering the material properties. It is clearly shown that the p/Y ratio of LJ-model reaches up to 2.61 at the inception of fully plastic regime without considering the material properties.

From Fig. 14 it is clearly known that the estimated p/Y value from LJ-model is higher than the value corresponding to KE-model upto the interference value around 60 after that the value from LJ-model is lower than the same obtained from KE-model upto the interference of inception of plastic regime. The KE-model p/Y value is 2.61% higher than that of LJ-model. The CEB model mean contact pressure is under estimated as compared with KE and LJ models. So for further comparison the KE and LJ models to be considered.
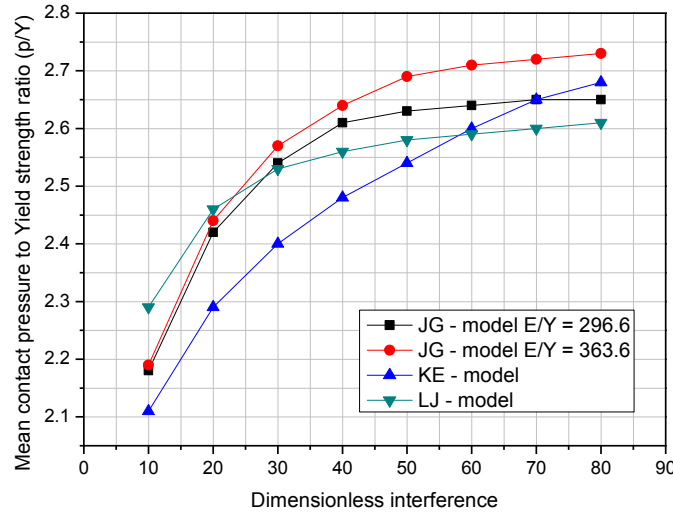
Fig. 15 Mean contact pressure to yield strength ratio Vs dimensionless interference (KE, LJ and JG model)

6.2 Analysis of JG-Model

From the JG-model in Eq. (4) the value of mean contact pressure to yield strength ratio are calculated and shown in the Table 5 upto an interference value of inception of fully plastic regime i.e., ω/ω_c=80. The JG-model proposed that it is fully material dependent.

From the above Table 5, It is clearly shown that the material *E/Y*=470 shows the different contact phenomena such as the p/Y value is greater as compared to *E/Y*=296.6 and 363.6. The p/Y value of material if *E/Y*=150 never reaches the value 2.61 as proposed by LJ-model. So for further comparison the material *E/Y*=296.6 and 363.6 is to be considered.

6.3 Comparison of KE, LJ and JG Models

The comparison has been made between material independent and material dependent models to analysis the behaviour of the elastic-plastic material by comparing the mean contact pressure and dimensionless interference. The main objective of this work is to predict the material range for analysing the elastic-plastic model by considering the properties of the materials. From the Tables 4 and 5 the values are taken for the comparison. From JG model the material *E/Y*=296.6 and 363.6 is considered for this study.

Fig. 15 shows the relation between mean contact pressure to yield strength ratio for KE, LJ and JG models upto the dimensionless interference 80. The material *E/Y*=363.6 shows the different contact phenomena such as the p/Y value reached 2.73. For material *E/Y*=296.6 the p/Y value reached 2.65 (close to 2.61) as proposed by LJ-model.

7. Conclusions

The performance for sphere and flat contact model and wheel - rail contact has been studied for

different *E/Y* values of material in the elastic-plastic region. The study was carried out on both simulation and analytical basic models. The simulation results of these contact models shows that the stress and strain distribution increases upto the *E/Y*=296.6 and again decreases with increases in the *E/Y* value. For further increase in *E/Y* value the stress and strain values are also increases. It shows that the contact analysis is not completely independent of material characteristics in the elastic-plastic region. The study has been made for the various flattening models and the mean contact pressure is compared. The ratio of the mean contact pressure to the yield strength ratio never reaches 2.6. The study has been made in this aspect the ratio of mean contact pressure to yield strength is calculated as 2.65 for the material *E/Y*=296.6 for the dimensionless interference ratio 80 in JG-model. It is concluded that, the critical value of *E/Y* has been identified as *E/Y*=296.6.

References

Arslan, M.A. and Kayabaşı, O. (2012), "3-D rail-wheel contact analysis using FEA", *Adv. Eng. Softw.*, **45**, 325-331.

Braghin, F., Lewis, R., Dwyer-Joyce, R.S. and Bruni, S. (2006), "A mathematical model to predict railway wheel profile evolution due to wear", *Wear*, 261, 1253-1264.

Chang, W.R., Etsion, I. and Bogy, D.B. (1987), "An elastic-plastic model for the contact of rough surfaces", *ASME. J. Tribol.*, **109**, 257-263.

Davis, J.R. (1999), *Metals Handbook*, 2nd Edition, ASM International, Metals Park, OH.

Donzella, G. and Petrogalli, C. (2010), "A failure assessment diagram for components subjected to rolling contact loading", *Int. J. Fatig.*, **32**(2), 256-268.

Haines, D.J. and Ollerton, E. (1963), "Contact stress distribution on elliptical contact surfaces subjected to radial and tangential forces", *Proceedings of Institution of Mechanical Engineers*, **177**(4), 45-54.

Jackson, R.L. and Green, I. (2005), "A finite element study of elasto plastic hemispherical contact against a rigid flat", *ASME. J. Tribol.*, **127**, 343-54.

Johnson, K.L. (1985), *Contact Mechanics*, Cambridge University Press, Cambridge.

Kogut, L. and Etsion, I. (2002), "Elastic-plastic contact analysis of a sphere and a rigid flat", *ASME. J. Tribol.,* 69, 657-662.

Kumaravelan, R., Ramesh, S., Sathish Gandhi, V.C., Joemax Agu, M. and Thanmanaselvi, M., (2013), "Analysis of multi leaf spring based on contact mechanics-a novel approach", *Struct. Eng. Mech.*, **47**(3), 443-454.

Mohan, P.M. (2012), "Analysis of railway wheel to study thermal and structural behaviour", *Int. J. Scientif. Eng. Res.*, **3**(11), 1-4.

Monfared, V. (2011), "A new analytical formulation for contact stress and prediction of crack propagation path in rolling bodies and comparing with finite element model (FEM) results statically", *Int. J. Phys. Sci.*, **6**(15), 3589-3594.

Monfared, V. (2012), "Contact stress analysis in rolling bodies by finite element method (FEM) statically", *J. Mech. Eng. Autom.*, **2**(2), 12-16.

Monfared, V. and Khalili, M.R. (2011), "Investigation of relations between atomic number and composition weight ratio in PZT and SMA and prediction of mechanical behavior", *Acta phys. Pol. A.*, **120**, 424-428.

Polin, L. and Lin, J.F. (2006), "A new method for elastic-plastic contact analysis of a deformable sphere and a rigid flat", *ASME. J. Tribol.,* 128, 221-229.

Sackfield, A. and Hills, D. A. (1983), "Some useful results in the classical Hertz contact problem", *J. Strain Anal.*, **18**(2), 101-105.

Santamaria, J., Vadillo, E.G. and Oyarzabal, O. (2009), "Wheel-rail wear index prediction considering multiple contact patches", *Wear*, **267**, 1100-1104.

Smith, J.O. and Liu, C.K. (1953), "Stresses due to tangential and normal loads on an elastic solid with application to some contact stress problems", *J. Appl. Mech.,* **20**, 157-166.

Sathish Gandhi, V.C., Ramesh, S., Kumaravelan, R. and Thanmanaselvi, M. (2012), "Contact analysis of spherical ball and a deformable flat model with the effect of tangent modulus", *Struct. Eng. Mech.*, **44**(1), 61-72.

Yaylac, M. and Birinci, A. (2013), "The receding contact problem of two elastic layers supported by two elastic quarter planes", *Struct. Eng. Mech.*, **48**(2), 241-255.

Zakeri, J.A., Fathali, M. and Boloukian, N. (2011), "Effects of rail cant on wheel-rail contact forces in slab tracks", *Int. J. Mech. Appl.*, **1**(1), 12-21.

Zhu, J.J., Ahmed, A.K.W. and Rakheja, S. (2007), "An adaptive contact model for simulation of wheel-rail impact load due to a wheel flat", *Proceedings of the 13th National Conference on Mechanisms and Machines*, IISc, Bangalore, India.

Zong, N. and Dhanasekar, M. (2012), "Analysis of rail ends under wheel contact loading", *Int. J. Aeros. Mech. Eng.*, **6**, 452-460.

CC

Nomenclature

Y	-	Yield Strength	N/mm^2
P^*	-	Dimensionless load	-
A^*	-	Dimensionless area	-
υ	-	Poisson's ratio	-
ω^*	-	Dimensionless interference	-
ω	-	Interference	mm
ω_c	-	Critical interference	mm
E	-	Young's modulus	N/mm^2
E/Y	-	Young's modulus to Yield strength ratio	-
P_m	-	Mean contact pressure (CEB - model)	N/mm^2
P	-	Mean contact pressure (JG- model)	N/mm^2
p	-	Mean contact pressure (KE - model)	N/mm^2
H	-	Hardness coefficient	-